ACTS
Mobile Telecommunications Summi

Granada, Spain
November 27-29 1996

Performance Analysis of a DCQPSK-OFDM Modem Using Analog BB Filters

M.Gabriella Di Benedetto and Paolo Mandarini

Universita' di Roma "La Sapienza" Dip. INFOCOM, via Eudossiana 18, 00184 Rome, Italy.
e-m: gaby@acts.ing.uniroma1.it, paolo@acts.ing.uniroma1.it

Abstract: *Results of a performance analysis on a DCQPSK-OFDM system using analog BB filters is presented. The above system configuration is typically affected by a mismatch of the I and Q paths. As regards the transmitter side, theoretical analysis show that the mismatch can be represented by a mismatch transfer function. The maximum amplitude/phase mismatcth of the BB filters paths and the maximum phase error of the in-phase and in-quadrature carriers are reported.*

Introduction

In this paper, a performance analysis on a DCQPSK-OFDM system is carried out. In this system, the reference axis for each submodulator is constituted by the phase of the previous (in frequency) submodulator[1]. In a system such as the Median system which is characterized by a high system clock, analog base-band filters must be used, and the effects produced by the mismatch between the in-phase (I) and in-quadrature (Q) filters must be analyzed. Section 1 describes the modem operations of a full-digital QPSK/OFDM modem. In section 2, the add-on necessary to realize a DC scheme are reported and the error probability is evaluated. In section 3, the effects of the mismatch between I and Q baseband paths are examined. Finally, section 4 contains the applications and section 5 the conclusions.

1. Description of a QPSK OFDM modem.

The Orthogonal Frequency Division Multiplex is a digital modulation scheme in which several digitally modulated signals are frequency multiplexed. Each modulator uses the same modulation method (QAM, CPSK or DCPSK), the same symbol period T_s, the same rectangular data pulse, and carries β bits/symbol. The subcarrier frequencies of the modulators are spaced by Δf around the carrier frequency f_p; moreover, the symbol period must be greater than $T_o = 1/\Delta f$, and is usually written as $T_s = T_o+T_g$, in which T_g is a *guard time* which is introduced to cope with defective symbol synchronization and multipath. Other important parameters of the OFDM modem are the number N of available subcarriers (a power of two) and the number $N_u = M_1 + M_2 < N$ of effectively used subcarriers (M_1 is the number of subcarriers at frequencies above the system carrier, M_2 -1 is the number of subcarriers below the system carrier). A full-digital implementation of the OFDM scheme, based on the use of IFFT/FFT processors ([1],[2], Fig.1), produces a sequence of $N+N_g$ samples for each OFDM symbol, taken *exactly* at frequency B, where $N_g = T_g \cdot B$ is the number of samples belonging to the prefix. Figure 2 represents the BB equivalent of the overall analog connection, in which an eventual mismatch between the in-phase and in-quadrature paths of the transmitter is highlighted.

In a QDCPSK-OFDM system, the samples of the complex envelope of the transmitted signal are generated by an IFFT processor from a sequence of $N_u < N$ constellation points $\{c_{-M_2-1},..,c_0,..,c_{M_1}\}$. The sequence $\{c_m\}$ is generated by a segmenter & differential encoder described in the next section, from the input binary data sequence. In the present section, we suppose

[1] This scheme is used in "burst mode" transmissions, in which previous (in time) OFDM symbols can be transmitted by different users.

$H_{BTI}(f) = H_{BTQ}(f) \equiv H_{BT}(f)$ and $\phi = 0$; therefore, the received complex envelope, and its Fourier Transform are given by:

$$y(t) = \sum_{k=-N_g}^{N-1} d_k \cdot g(t - k/B) \Leftrightarrow Y(f) = G(f) \cdot \sum_{k=-N_g}^{N-1} d_k \cdot e^{-j2\pi f \frac{k}{B}} \tag{1}$$

where:

$$g(t) \equiv \pi(t) * h(t) \Leftrightarrow G(f) = \frac{1}{B}\frac{sin(\pi f / B)}{\pi f / B} \cdot H_{BT}(f) \cdot H_R(f) \equiv G_T(f) \cdot H_{BR}(f) \tag{2}$$

$$\pi(t) = rect \text{ waveform from each DAC} \Leftrightarrow \frac{1}{B}\frac{sin(\pi f / B)}{\pi f / B} \equiv \Pi(f)$$

$$d_k = \text{IFFT of } \{D_m\} = \sum_{m=0}^{N-1} D_m e^{j2\pi \frac{mk}{N}} \text{ periodic of period } N \qquad D_m = \begin{cases} c_m & 0 \le m \le M_1 \\ 0 & M_1 < m \le N - M_2 \\ c_{m-N} & N - M_2 < m \le N-1 \end{cases} \tag{3}$$

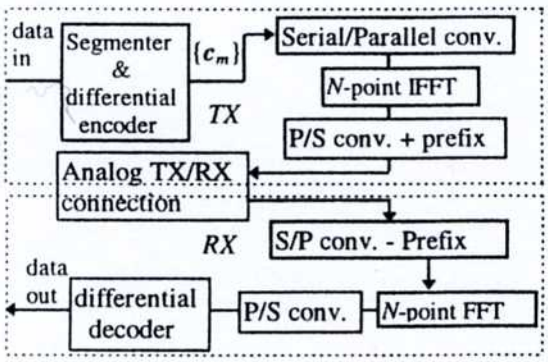

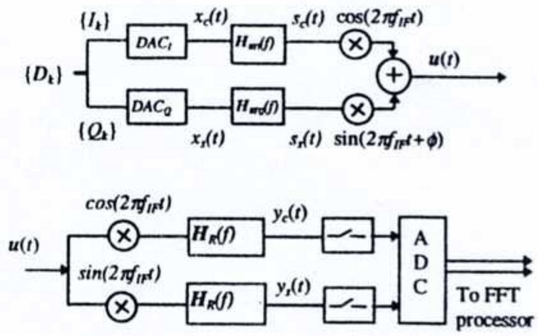

Fig.1 Block diagram of an OFDM modem.

Fig.2 Block diagram of the baseband equivalent of the analog TX/RX connection.

The signal $y(t)$ is sampled at frequency $B = N \cdot \Delta f$. If the duration of the impulse response $g(t)$ is lower than T_g, the m-th FFT output, i.e. an estimate of the transmitted constellation point c_m, is given by: $\hat{c}_m = G(m \cdot \Delta f), -M_2 < m \le M_1$. Therefore, the estimate of c_m is biased by $\beta_m = G(m\Delta f)$. In a CPSK scheme, the phase of β_m may destroy the information carried by the modulation; this can be avoided by using a differentially coherent scheme[2], as described in the next section.

2. Error probability in a QDCPSK/OFDM system.

It is hypothesized that an additive gaussian noise with a symmetrical power density N_o is present at the channel output. Therefore, a complex zero mean gaussian process $n(t)$, with symmetric power spectrum $P_N(f) = 4N_o$ is added to the complex envelope of the received signal $y(t)$. This noise produces an additive zero mean gaussian complex noise sample n_k on each FFT output, with variance ([1]):

$$\psi_m^2 = \frac{B}{N} P_N(m \cdot \Delta f) = 4N_o |H_R(f_m)|^2 \Delta f \tag{5}$$

The data sequence is grouped into dibits and coded using a 4 points constellation represented in Fig.3, to produce a sequence $\{p_k\}$ which is then differentially encoded to generate a sequence $\{q_k\}$ such that $q^*_{m-1} \cdot q_m = p_m$. Each term of $\{q_k\}$, which belongs to a set of 8 values equally spaced along the unitary circle, is multiplied by a precorrection factor $\gamma_k = 1/G_T(f_k)$INCRUSTAR which equalizes the SNR on each subcarrier, to produce the transmitted constellation sequence $c_k = q_k/G_T(f_k)$. Therefore, the received signal power, which is half the power of its complex envelope, is given by:

$$P_R = \frac{1}{2}\sum_{k=-\infty}^{\infty} E\left\{|d_k|^2\right\}|G_T(f_k)|^2 \cong \frac{1}{2}\sum_{k=-M_2}^{M_1} |\gamma_k|^2 |G_T(f_k)|^2 = \frac{N_u}{2} \tag{6}$$

Finally, we indicate by SNR the ratio between the received power and the noise power in a frequency band equal to the on-air symbol rate $f_s = N_u/T_s = N_u/T_o(1+T_g/T_o) = N_u\Delta f/(1+T_g/T_o)$. From (6), one has:

$$SNR = \frac{P_R}{2N_o f_s} = (1 + T_g / T_o)\frac{1}{4N_o\Delta f} \tag{7}$$

If the differential co/decoding is taken into account, the estimate of the transmitted constellation point p_m on the m-th subcarrier is:

$$\begin{aligned} \hat{p}_m &= c^*_{m-1} c_m = \{H^*_R(f_{m-1}) \cdot q^*_{m-1} + n^*_{m-1}\}\{H_R(f_m) \cdot q_m + n_m\} \\ &\cong H^*_R(f_{m-1}) \cdot H_R(f_m) \cdot p_m + H_R(f_m) \cdot q_m \cdot n^*_{m-1} + H^*_R(f_{m-1}) \cdot q^*_{m-1} \cdot n_m \equiv \beta_m p_m + v_m \end{aligned} \tag{8}$$

Equation (8) shows that the estimate of p_m is affected by an additive gaussian noise v_m and by a multiplicative bias $\beta_m = H^*_R(f_{m-1}) \cdot H_R(f_m) \equiv b_m \cdot e^{j\varphi_m}$, as in a coherent system, but now φ_m is usually small. Since n_m and n_{m-1} are independent and since $|q_m|=1$, from (8) the variance of v_m is: $\sigma_v^2 = (|H_R(f_m)|^2 + |H_R(f_{m-1})|^2) \cdot 4N_o |H_R(f_m)|^2 \Delta f$. Finally, since $p_m = (\pm 1 \pm j)/\sqrt{2}$, the bit error rate on the k-th constellation point is:

[2] In effect, a CPSK scheme requires the use of an equalization procedure, but it is prohibitive in a multi-user burst-mode operations.

$$P_m = \frac{1}{4} erfc(z_{m+}) + \frac{1}{4} erfc(z_{m-}) \tag{9}$$

$$z_{m\pm}^2 = \left\{ \frac{b_m(\cos\varphi_m \pm sin\varphi_m)}{\sqrt{2}\sigma_v} \right\}^2 = \frac{\left|H_R(f_{m-1})\right|^2 \cdot (\cos\varphi_m \pm sin\varphi_m)^2}{8N_o\Delta f\left\{\left|H_R(f_m)\right|^2 + \left|H_R(f_{m-1})\right|^2\right\}} \cong \frac{(\cos\varphi_m \pm sin\varphi_m)^2}{8N_o\Delta f} = \frac{SNR \cdot (\cos\varphi_m \pm sin\varphi_m)^2}{4(1+T_g/T_o)}$$

3. Effect of LP transmitter filters mismatch on the I and Q paths.

In Fig.2, the input sequence to be transmitted is represented by two real sequences $\{ I_{-N_g}, \ldots, I_{N-1} \}$ and $\{ Q_{-N_g}, \ldots, Q_{N-1} \}$ which are D to A converted, filtered and cos/sin modulated. We indicate by :

$$G_{TI}(f) = \frac{1}{B} \frac{sin(\pi f / B)}{\pi f / B} H_{BTI}(f) \cdot H_T(f) \Leftrightarrow g_{TI}(t) \tag{10}$$

$$G_{TQ}(f) = \frac{1}{B} \frac{sin(\pi f / B)}{\pi f / B} H_{BTQ}(f) \cdot H_T(f) \Leftrightarrow g_{TQ}(t)^3 \tag{11}$$

the equivalent LP filters of the I and Q paths, respectively. The RF signal can be represented by:

$$s(t) = s_c(t) \cdot \cos(2\pi f_p t) - s_s(t) \cdot \sin(2\pi f_p t + \phi) = s_I(t) \cdot \cos(2\pi f_p t) - s_Q(t) \cdot \sin(2\pi f_p t)$$
$$s_I(t) = s_c(t) - \sin\phi \cdot s_s(t)$$
$$s_Q(t) = \cos\phi \cdot s_s(t)$$
$$s_c(t) = \sum_{k=-N_g}^{N-1} I_k \cdot g_{TI}(t - k/B)$$
$$s_s(t) = \sum_{k=-N_g}^{N-1} Q_k \cdot g_{TQ}(t - k/B) \tag{12}$$

or by the Fourier Transform of its complex envelope $s(t) = s_I(t) + js_Q(t)$:

$$S(f) = G_{TI}(f) \sum_{k=-N_g}^{N-1} I_k \cdot e^{-j2\pi fk/B} + je^{j\phi} G_{TQ}(f) \sum_{k=-N_g}^{N-1} Q_k \cdot e^{-j2\pi fk/B}$$

[3] Any difference between the true DAC's output pulse waveform and the ideal *rect* function is included in the H_{BTI} and H_{BTQ} transfer functions.

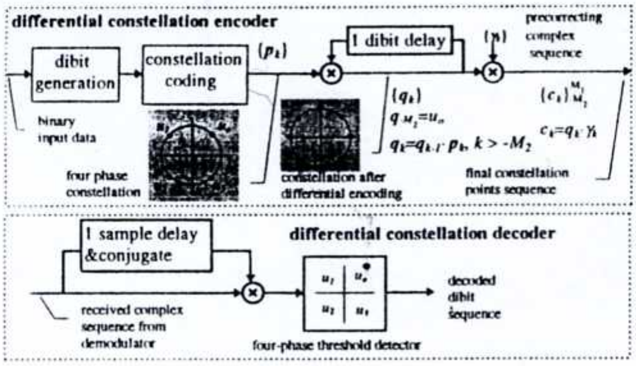

Fig.3 Block diagram of the differential co/decoder

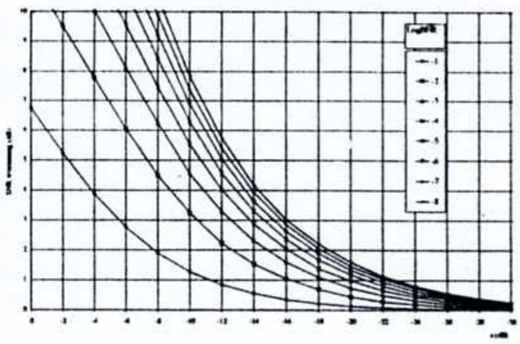

Fig.4 SNR worsening versus a (dB), for different values of $\log_{10}$(Bit Error Probability) evaluated @ a = 0.

If one sets:

$$\begin{cases} G_{TI}(f) \equiv G_T(f) + G_e(f) \\ G_{TQ}(f) \equiv G_T(f) - G_e(f) \end{cases} \Rightarrow \begin{cases} G_T(f) = \left(G_{TI}(f) + G_{TQ}(f)\right)/2 \\ G_e(f) = \left(G_{TI}(f) - G_{TQ}(f)\right)/2 \end{cases} \tag{13}$$

one obtains:

$$\begin{aligned} S(f) &= G_T(f)\sum_{k=-N_g}^{N-1}(I_k + jQ_k)\cdot e^{-j2\pi fk/B} + G_e(f)\sum_{k=-N_g}^{N-1}(I_k - jQ_k)\cdot e^{-j2\pi fk/B} = \\ &= G_T(f)\sum_{k=-N_g}^{N-1} d_k \cdot e^{-j2\pi fk/B} + G_e(f)\sum_{k=-N_g}^{N-1} d_k^{*}\cdot e^{-j2\pi fk/B} \end{aligned} \tag{14}$$

The previous equations show that the mismatch between the *I* and *Q* LP paths adds a conjugate component to the transmitted sequence. Therefore, the *m*-th outputs of the FFT processor due to the first and second component, are given by:

$$\hat{c}_m^{(I)} = H_R(f_m)\cdot G_T(f_m)\cdot c_m = H_R(f_m)\cdot G_T(f_m)\cdot \gamma_m \cdot q_m \tag{15}$$

$$\hat{c}_m^{(Q)} = H_R(f_m)\cdot G_e(f_m)\cdot c_{-m}^{*} = H_R(f_m)\cdot G_e(f_m)\cdot \gamma_{-m}^{*}\cdot q_{-m}^{*} \tag{16}$$

respectively[4], and if we keep the ideal choice $\gamma_k = 1/G_T(f_k) = \gamma^{*}_{-k}$ [5], from the linearity of the demodulation process, the true *m*-th output is:

[4] We have also used the following relation: $\sum_{k=0}^{N-1} D_k^{*} e^{-j2\pi nm/N} = \left(\sum_{k=0}^{N-1} D_k e^{j2\pi nm/N}\right)^{*} = d_{-m}^{*} = d_{N-m}^{*}$

[5] We have supposed that the IF/RF transmitting filters exibit an aritmetic symmetry around the carrier frequency.

$$\hat{c}_m = \hat{c}_m^{(I)} + \hat{c}_m^{(Q)} = H_R(f_m)\cdot\left(q_m + \frac{G_e(f_m)}{G_T(f_m)}\cdot q_{-m}^*\right) \equiv H_R(f_m)\cdot\left(q_m + H_e(f_m)\cdot q_{-m}^*\right) \qquad (17)$$

where:

$$H_e(f_m) \equiv \frac{G_e(f)}{G_T(f)} = \frac{G_{TI}(f) - G_{TQ}(f)}{G_{TI}(f) + G_{TQ}(f)} = \frac{H_{BTI}(f) - e^{j\phi} H_{BTQ}(f)}{H_{BTI}(f) + e^{j\phi} H_{BTQ}(f)} \qquad (18)$$

Equation (18) shows that any *mismatch* between the LP filters in the *I* and *Q* paths causes an *additive* error component which depends upon a different transmitted point and on the relative difference $H_e(f_m)$ between the two LP filter frequency behaviors (and *not* from the IF filter behavior). After the differential decoding, without noise and supposing $H_e(f_m) << 1$, one has :

$$\begin{aligned}
\hat{p}_m &= c_{m-1}^* c_m = H_R^*(f_{m-1}) H_R(f_m) \{q_{m-1}^* + H_e^*(f_{m-1})\cdot q_{-m-1}\}\cdot\{q_m + H_e(f_m)\cdot q_{-m}^*\} \\
&\equiv G_o^*(f_{m-1}) G_o(f_m) \left\{ p_m + H_e(f_m)\cdot q_{m-1}^* q_{-m}^* + H_e^*(f_{m-1})\cdot q_m q_{-m-1} \right\} = \\
&\equiv G_o^*(f_{m-1}) G_o(f_m) \left\{ \gamma_{m-1}^* \gamma_m p_m + H_e(f_m)\cdot \varepsilon_m + H_e^*(f_{m-1})\cdot \eta_m \right\} \equiv \beta_m p_m + \alpha_m
\end{aligned} \qquad (19)$$

where $\varepsilon_m \equiv q_{m-1}^* q_{-m}^* = e^{j\vartheta_m}$, $\eta_m \equiv q_m q_{-m-1} = e^{j\theta_m}$ and ϑ_m and θ_m take 8 different values, uniformly distributed along the round angle. Equation (19) shows that the estimate of p_m is affected by a multiplicative bias β_m and by an additive bias α_m. By applying the same procedure as in sec.2, each bit-decision on the *k*-th transmitted constellation point is affected by the following bit error probability :

$$P_m(\psi_m, \zeta_m) = \frac{1}{4} erfc(z_{m+}) + \frac{1}{4} erfc(z_{m-}) \qquad (20)$$

$$z_{m\pm}^2 = \frac{SNR}{4(1 + T_g / T_o)} \left[1 \pm \sqrt{2} a_m (\cos\psi_m + \cos\zeta_m)\right]^2$$

Finally, the mean error probability can be obtained by averaging (20) over ψ_m and ζ_m, which are random variables uniformly distributed over 0-2π. Figure 4 shows the SNR worsening due to the presence of the mismatch between the I and Q paths, represented by the corresponding value of $a = |H_e(f)|$ (in dB) and for different values of the error probability, evaluated for $a_{dB} = 0$. We conclude that if a worsening of 1 dB is accepted for every used subcarrier, the maximum value of a_{dB} is -23 dB.

4. Applications

4.1 Maximum amplitude/phase mismatch between the in-phase and in quadrature filters.

The effect of the amplitude/phase mismatch between the in-phase and the in-quadrature LP transmitter filters can be isolated by supposing $\varphi = 0°$. In this case, indicating by $a = |H_e(f)|$, one has:

$$a = \frac{\left\|\left[1 - \boldsymbol{H}_{BTQ}(f)/\boldsymbol{H}_{BTI}(f)\right]\right\|}{\left\|\left[1 + \boldsymbol{H}_{BTQ}(f)/\boldsymbol{H}_{BTI}(f)\right]\right\|} \equiv \left|\frac{1 - \Delta a_{BT}(f)\cdot e^{j\Delta\varphi_{BT}(f)}}{1 + \Delta a_{BT}(f)\cdot e^{j\Delta\varphi_{BT}(f)}}\right|, \text{ with: } \begin{array}{l} \Delta a_{BT}(f) \equiv \left|\boldsymbol{H}_{BTQ}(f)/\boldsymbol{H}_{BTI}(f)\right| \\ \Delta\varphi_{BT}(f) \equiv \arg\left\{\boldsymbol{H}_{BTQ}(f)/\boldsymbol{H}_{BTI}(f)\right\} \end{array}$$

Figure 5 shows the area in the $\{\Delta a_{(dB)}, \Delta\varphi_{(degree)}\}$ plane for which $20\log_{10} a < A_{dB}$. As a result, for A_{dB} = -23 dB, a maximum phase mismatch of 8° is possible only in the presence of a perfect amplitude matching (Δa= 0 dB); this mismatch is reduced to zero for an amplitude mismatch of 1.3 dB.

4.2 Effect of the phase error ϕ between the in-phase and in-quadrature transmitter carriers.

The effect of a phase error ϕ between the in-phase and in-quadrature transmitter carriers can be isolated by supposing $\boldsymbol{H}_{BTI}(f) = \boldsymbol{H}_{BTQ}(f)$. One obtains:

$$a_{dB} \equiv 20\log_{10}\left|\boldsymbol{H}_e(f)\right| = 20\log_{10}\left|\frac{1-e^{j\phi}}{1+e^{j\phi}}\right| \tag{21}$$

The behaviour of a_{dB} versus ϕ is shown in Fig. 6. This result can be combined with those presented in Fig.4: when a worsening of 1 dB on SNR it is imposed, it appears that the maximum phase error is 8°.

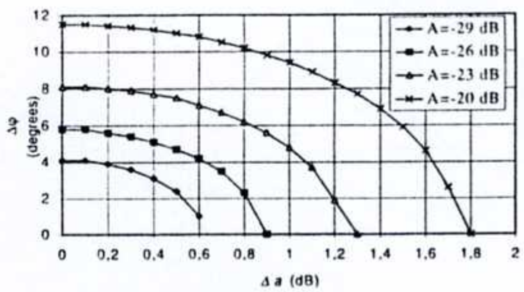

Fig.5 Locus of the points, in the plane $\{\Delta a_{(dB)}, \Delta\varphi_{(degree)}\}$

for which: $20\log_{10} a < A_{dB}$.

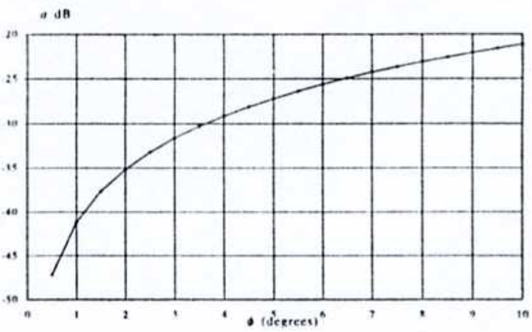

Fig.6 Behavior of a_{dB} versus ϕ [eq.(21)]

5. Conclusions

In this paper, the effects of a mismatch between the I and Q transmitter paths were examined. It was shown that the worsening effects of the mismatch can be taken into account by a mismatch function $\boldsymbol{H}_e(f)$, which must be limited for any accepted *SNR* worsening. On the basis of teoretical considerations, the maximum amplitude/phase mismatcth of the BB filters in the transmitter's LP paths and the maximum phase error of the in-phase and in-quadrature carriers were determined.

Future work will include mismatch effects on the receiver side.

References

[1] T. de Couasnon, R. Monnier, J.B. Rault, OFDM for digital TV broadcasting, Signal processing 39 (1994) I-32, pp. 1 -32.

[2] B. le Floch, M. Alard, C. Berrou, Coded Orthogonal Frequency Division Multiplex, Proc. IEEE, Vol.83, n. 6, 1995, pp 982-996.